Cumhuriyet Sci. J., 45(4) (2024) 718-728
DOI: https://doi.org/10.17776/csj.1419602

Cumhuriyet Science Journal

| csj.cumhuriyet.edu.tr | Founded: 2002 ISSN: 2587-2680 e-ISSN: 2587-246X Publisher: Sivas Cumhuriyet University

Utilization of Multiwalled Carbon Nanotubes as Adsorbent for Removal of Acid Violet 17 Dye: Equilibrium, Kinetics and Thermodynamic Studies

Neşe Keklikcioğlu Çakmak [1,a], İlknur Şentürk [2,b,*]

[1] *Department of Chemical Engineering, Faculty of Engineering, Sivas Cumhuriyet University, Sivas 58140, Türkiye*
[2] *Department of Environmental Engineering, Faculty of Engineering, Sivas Cumhuriyet University, Sivas 58140, Türkiye*
**Corresponding author*

Research Article

History
Received: 14/01/2024
Accepted: 07/09/2024

ABSTRACT

The adsorption capacity and separation efficiency of multiwalled carbon nanotube (MWCNT) were investigated for the removal of Acid Violet 17 (AV 17) dye in an aqueous solution. The effect of reaction conditions, such as contact time, AV 17 initial concentration, pH, adsorbent dosage, and temperature, on the adsorption capacity of MWCNTs was investigated. It was found that a contact time of 180 min, an adsorbent dosage of 0.8 g/L, and 100 mg/L AV 17 concentration are ideal conditions for maximum adsorption capacity (119.45 mg/g). AV 17 dye adsorption on MWCNTs followed a pseudo-second-order kinetic model (R^2 = 0.9998) and the Langmuir isotherm model (R^2 = 0.9813) suggesting that adsorption was the uniform and homogenous process. The maximum adsorption capacity from the Langmuir isotherm model was determined to be 322.58 mg/g. Adsorption of AV 17 dye was determined to be spontaneous and thermodynamically favorable since the values of ΔG^o were negative. Positive $\Delta H°$ and $\Delta S°$ values suggest that the process is endothermic and randomness. The research results showed the MWCNTs could be used successfully to remove dye for the water treatment process.

Keywords: Multiwalled carbon nanotube, Acid violet 17, Adsorption, Adsorption mechanism.

[a] nkeklikcioglu@cumhuriyet.edu.tr https://orcid.org/0000-0002-8634-9232 [b] ilknursenturk@cumhuriyet.edu.tr https://orcid.org/0000-0002-8217-2281

Introduction

Dyes, one of the largest and most important groups of chemicals, especially Azo group dyes, are widely used for textile and leather dyeing [1,2]. Dyes contain different compounds with toxic, carcinogenic, and mutagenic properties as well as unknown environmental behaviors [3]. For this reason, dyes originating from industrial discharges affect the natural beauty of the streams or rivers where the discharge is made and also have highly toxic and harmful effects on the flora and fauna in aquatic life [1]. Approximately 70% of all commercially used dyes are azo dyes, and approximately 20% of these dyes can enter wastewater and cause an environmental problem. Due to the health and environmental concerns associated with synthetic dyes, it is necessary to fully treat the dyes before discharge into natural water bodies [4].

The chemical oxygen demand is raised when dyes are present in the water structure. Light penetration into the water is impeded by its impact on the photosynthetic activities of aquatic plants. Dyes are hazardous even at very low doses, and treating them is highly challenging due to their complexity. Due to the stability of dyes against heat, light, and microbial attack, the desired efficiency cannot be achieved with conventional wastewater treatment methods. Therefore, appropriate technologies should be developed to protect the ecosystem [3]. Different methods such as sorption, chemical flocculation, flotation, sedimentation, chemical oxidation, filtration technologies, photocatalytic and electrochemical oxidation, and biological techniques are used to remove dyes from the solution before discharge into the natural environment. However, these techniques have some limitations such as secondary pollution formation and high cost. Among the different applicable techniques, adsorption is widely used for the removal of dyes from wastewater. The sorption process has a definite advantage over other methods used for dye recovery because it is a simple, selective, economical, and efficient process, does not generate hazardous by-products, and is flexible in operation [5,6].

Acid Violet 17 (AV 17), the model dye for this research, is an anionic azo dye. It is widely used in the paper, textile, food, and cosmetics industries. Since it is a dye related to the trimethyl methane class, it shows carcinogenic properties. Therefore, to avoid hazards caused by AV 17 in wastewater, this wastewater must be treated [4].

There are some previous studies conducted by researchers for the treatment of AV 17 dye. For example, Şentürk and Alzein [7] studied the adsorption of AV 17 with pistachio shells activated with 10% N H_2SO_4 and obtained 93.04% removal efficiency. The maximum Langmuir adsorption capacity (q_m) was determined as 26.455 mg/g for 160 mg/L AV 17. In another study, biosorbents obtained from the activation of fallen leaves of *Ficus racemosa* with NaOH and H_2SO_4 were used for the adsorption of AV 17 dye. The q_m value for raw biosorbent, H_2SO_4-activated biosorbent, and NaOH-activated biosorbent was determined as 45.25, 61.35, and 119.05 mg/g respectively [8]. Thinakaran vd., [9] studied the

removal of AV 17 dye by activated carbon prepared from sunflower seed shells. The q_m value of the adsorbent was 65.78 mg/g. Jain vd., [5] synthesized a new adsorbent from *Salvadora persica* powder by chemical activation to remove AV 17 from aquatic solution. The q_m values for raw and activated adsorbent were determined as 74.28 and 141.30 mg/g, respectively.

Carbon nanotubes (CNTs) have become a novel adsorbent for the removal of dyes from wastewater in recent times. Carbon nanotubes, which consist of both single-walled and multiwalled carbon nanotubes (SWCNTs and MWCNTs), are hexagonal lattice-shaped cylindrical nanostructures with a large specific surface area (100–1000 m^2g^{-1}) that are primarily made of carbon atoms in sp^2 hybridization [10]. The physical characteristics of the nanomaterial and the structure of the adsorbed dye determine how dyes adsorb on carbon nanotubes. Because of CNTs unique chemical structure, large specific surface area, small sizes, layered and hollow structure, abundant adsorption sites, easy attachment of functional groups, and the ability to be decorated with other nanoparticles. They are a desirable substitute for eliminating dyes, fluoride, heavy metals, and other organic and inorganic pollutants from wastewater and water [11,12].

The present investigation aims to explore the adsorption behavior and removal capacity of MWCNTs, and other operating parameters affecting the adsorption of AV 17 from aquatic solution. In batch experimental studies, parameters known to affect adsorption efficiency were investigated. Isotherm, kinetic, and thermodynamic models were calculated to investigate the adsorption mechanism, to understand the process kinetics, and to see the effect of temperature on the process. So far, many researchers have reported the removal of different dyes and pollutants from aqueous solution by a multiwalled carbon nanotube nanocomposite. They investigated adsorption kinetics, the adsorption capacity of the adsorbent, and the effects of adsorption dosage and solution pH values on removal efficiency. However, these studies were carried out at lower concentrations with cationic azo dyes. This study differs in terms of investigating the treatment of high concentrations of AV 17, an anionic azo dye, with MWCNT.

Material and Method

Adsorbent

Analytical-grade chemicals were all employed in this investigation. Multi walled carbon nanotubes (MWCNTs) were used exactly as they were received from Nanografi (Turkey), with an average outside diameter of 8–28 nm.

Preparation of the Dye Solution

Acid Violet 17, an anionic azo dye, was selected for this study. The chemical structure and properties of AV 17 dye are shown in Figure 1. The dye was weighed and dissolved in distilled water and the stock dye solution at a concentration of 1 g/L was diluted to the desired working concentrations and used in batch experiments.

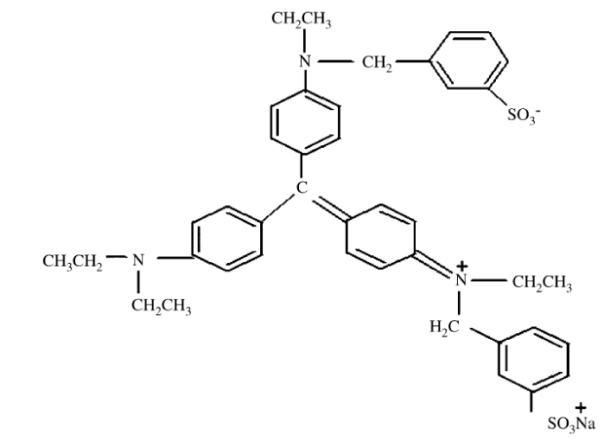

CF: $C_{41}H_{44}N_3NaO_6S_2$ MW: 761.93 g/mol λ_{max} = 542 nm

Figure 1. Molecular structure and properties of AV 17 [7].

Adsorption Experiments

Experimental studies were carried out in a 10 mL glass tube at room temperature (25°C). Batch experiments consisted of contact time, pH, adsorbent dosage, initial dye concentration, and temperature studies. The time-dependent behavior of dye adsorption was studied by varying the adsorption time. The natural pH of the prepared dye solution was measured as 6.52. Glass tubes containing the prepared mixture were placed in an incubator shaker (Gerhardt, Germany) and stirred at 150 rpm at 25°C. Each test tube was then analyzed separately at the time intervals determined for the analysis to determine the concentrations of unadsorbed dye. Adjustments required during the pH study were carried out with dilute HCl and/or NaOH solutions. Other experimental conditions are given in Table 1.

Table 1. Batch experimental conditions

Experiment	Solution pH	Adsorbent dosage (g/L)	Initial AV 17 conc. (mg/L)	Contact time (hours)	Temperature (°C)
Adsorbent concentration	6.52	0.1-1.0	100	3	25
Effect of pH	2-12	0.8	100	3	25
Effect of time	6.52	0.8	100	5-330 min	25
Effect of concentration	6.52	0.8	100-300	3	25
Effect of temperature	6.52	0.8	200	3	25-35-45-55

After the contact time was determined in all experimental studies, the loaded MWCNT adsorbent was centrifuged at 4000 rpm for 5 min and separated from the solution. The filtrate was then analyzed using a UV/Vis

spectrophotometer (Spectroquant Pharo 300, Merck) at a maximum wavelength of 542 nm and the concentrations of AV 17 remaining in the solution were determined. The adsorption efficiency (%) and adsorption capacity (q_e, mg/g) of the adsorbent used in the study were calculated as given below.

$$\text{Adsorption efficiency, R (\%)} = \frac{Co-Ce}{C_o} * 100 \quad (1)$$

$$\text{Adsorption capacity } (q_e) = [(C_o\text{-}C_e) * V] / m \quad (2)$$

Where,

q_e: Adsorption capacity of the adsorbent (mg/g),

V: Solution volume (L),

C_o: Initial AV 17 concentration in the solution (mg/L),

C_e: Concentration of AV 17 remaining in the solution after treatment (mg/L),

m: Adsorbent quantity (g).

Results and Discussion

Characterizations of MWCNTs

SEM and EDX analysis

The surface morphology of MWCNTs was characterized by scanning electron microscopy (SEM).

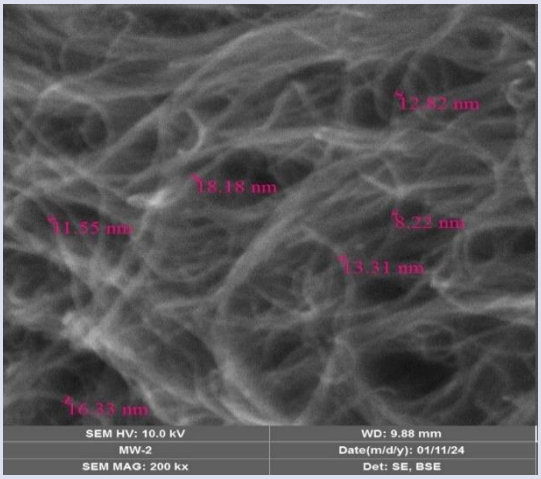

(a)

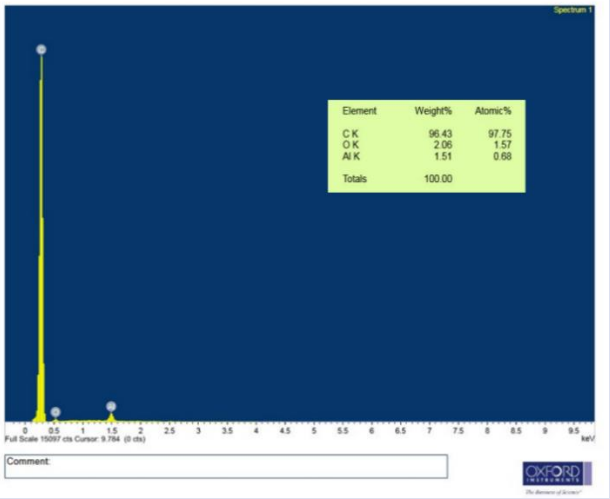

(b)

Figure 2. (a) SEM image of MWCNT (b) EDX spectra of MWCNT before the adsorption of AV 17 dye.

Figure 2 shows the MWCNTs' SEM and EDX images. The image indicates clearly that the MWCNTs are curved, twisted together, and cylindrical. As seen in Figure 2(a), MWCNTs have lengths ranging from several to tens of nanometers and diameters between 8 and 18 nm.

The presence of groups on the surface of carbon nanotubes is quantitatively analyzed using energy-dispersive X-ray spectroscopy (EDX) measurement. Figure 2(b) demonstrates the results of the MWCNTs. The data indicates that the sample contains oxygen in addition to carbon.

Figure 3 shows the SEM image and EDX result of MWCNT after AV 17 dye adsorption. When compared with the pre-adsorption image of MWCNT, it was observed that the spaces in the fibrous structure of MWCNT were filled. In the EDX result after adsorption, Na, Al and S peaks caused by AV 17 ($C_{41}H_{44}N_3NaO_6S_2$) dye are observed. SEM and EDX results show that MWCNT adsorbed AV 17 dye.

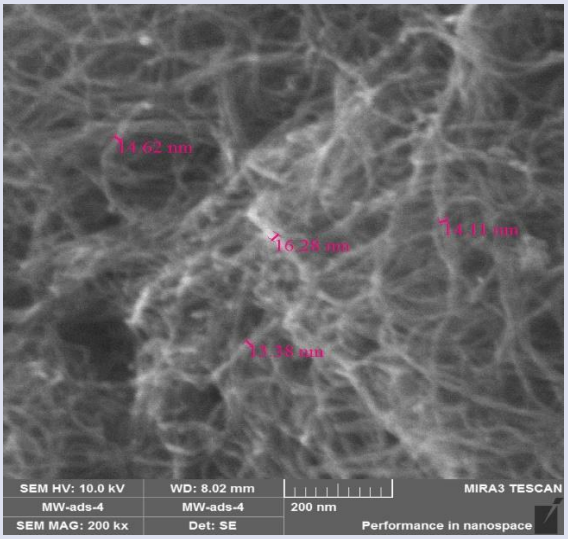

(a)

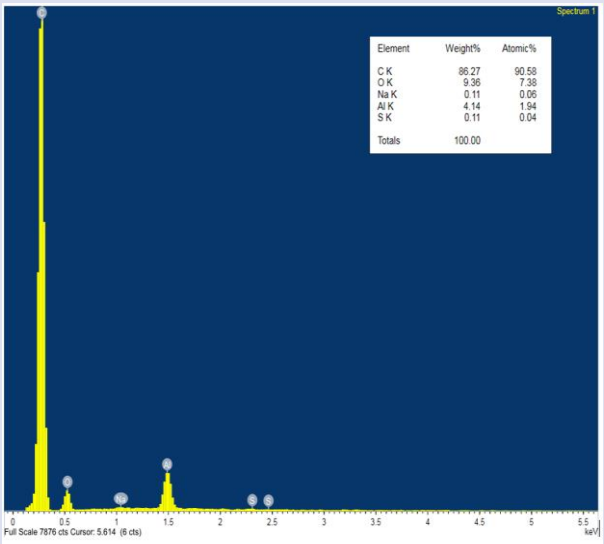

(b)

Figure 3. (a) SEM image of MWCNT (b) EDX spectra of MWCNT after the adsorption of AV 17 dye.

XRD analysis

The XRD pattern of the MWCNTs is shown in Figure 4. The diffraction patterns of typical graphite (002), (100), (004), and (110) are attributed to the intense diffraction peak around 2θ = 26° and the low intense diffraction peaks about 44°, 54°, and 79° in the pattern. The MWCNT XRD graph and results are consistent with previous research.

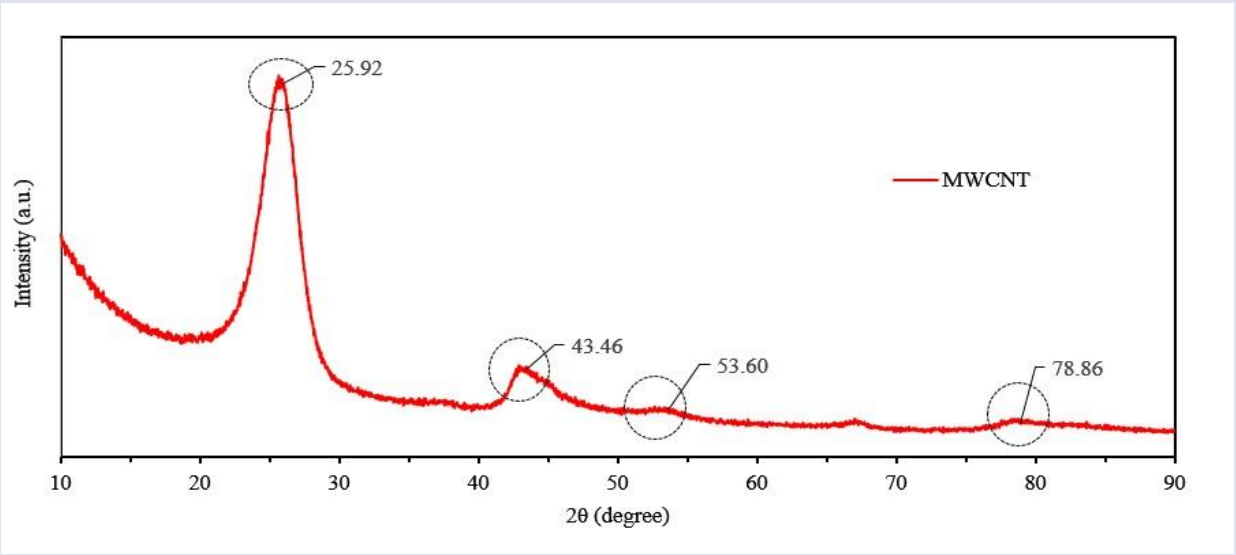

Figure 4. XRD patterns of MWCNT.

Adsorption studies

To investigate the adsorption behavior of AV 17 dye on the MWCNT adsorbent selected for this study, the effect of parameters such as contact time, pH, adsorbent amount, dye concentration, and temperature were investigated and the results were presented in detail.

Effect of adsorbent dosage

The unquestionably effective parameter in the adsorption process is the amount of adsorbent used in the solution. The adsorption of dye molecules becomes easier as the active adsorbent sites increase when the adsorbent dosage increases [13]. However, a further increase in the amount of adsorbent after a certain dose does not show a significant change in dye adsorption. In the study investigating Reactive Black 5 adsorption with Fe_3O_4@Granite magnetic adsorbent, results supporting this information were reported [13].

To investigate the effect of adsorbent dosage on AV 17 dye removal, the results obtained in the adsorption study at 100 mg/L initial AV 17 dye concentration are given in Figure 5. As the amount of adsorbent increased between 0.1 and 1.0 g/L, the dye removal increased because the effective surface area also increased. However, it was observed that the increase in dye removal was quite insignificant in adsorbent applications above 0.8 g/L (Figure 5). Therefore, the most suitable adsorbent amount was determined as 0.8 g/L MWCNT.

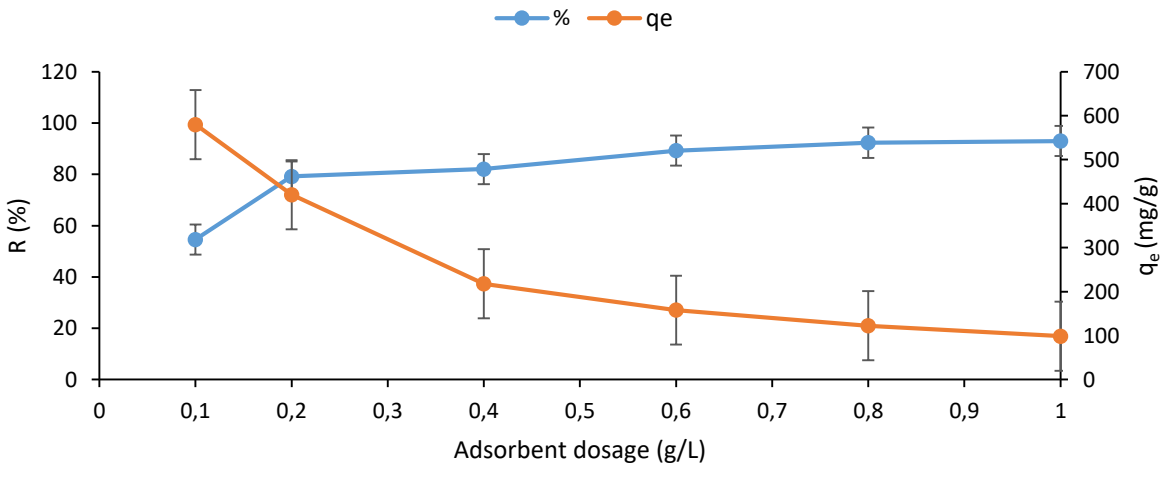

Figure 5. Effect of adsorbent amount on adsorption capacity and removal efficiency.

Effect of initial dye concentration

To investigate the effect of initial AV 17 dye concentration on adsorption, the five different dye concentrations (100, 150, 200, 250, and 300 mg/L) with 0.8 g/L adsorbent dosage were studied (Figure 6). After the study, it was observed that MWCNT treatment efficiency decreased with increasing dye concentration. At 100 mg/L AV 17 concentration, 91.64% dye removal efficiency was obtained, while the efficiency was 73.3% at 300 mg/L dye concentration. It is seen that the decrease in yield is faster after 250 mg/L AV 17 concentration. As the dye concentration increases, the treatment efficiency decreases as the pores and surface saturation of the adsorbent increase [14]. However, adsorption capacity increased with increasing dye concentration. The MWCNT adsorbent's adsorption capacity rose from 121.62 mg/g to 270.36 mg/g when the AV 17 dye concentration was raised from 100 mg/L to 250 mg/L.

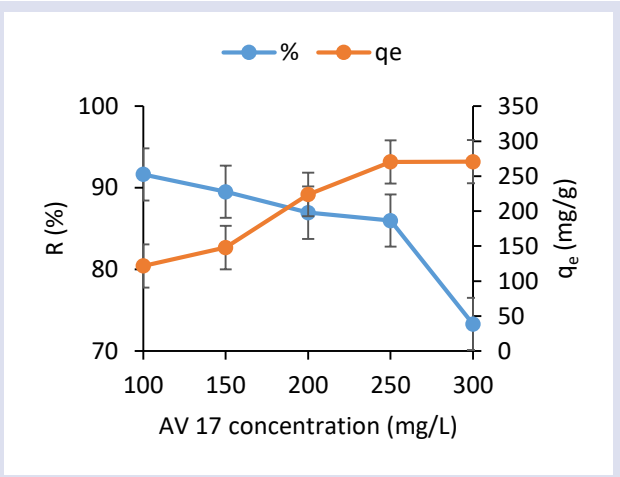

Figure 6. Effect of AV 17 dye concentration on adsorption capacity and removal efficiency.

Effect of contact time

The effect of different contact times on adsorption with MWCNT at 100 mg/L AV 17 concentration under the experimental conditions given in Table 1 was investigated and the results are shown in Figure 7. As can be seen from Figure 7, the treatment started in the first minutes of the contact time and a rapid treatment was realized for the first 120 minutes. At the end of 180 minutes, it was observed that the adsorption process reached equilibrium. The removal efficiency of MWCNT adsorbent was 90% and the adsorption capacity was 119.45 mg/g at the assumed equilibrium moment. The adsorption rate, which occurs in the first minutes and then stops or slows down, shows that there is plenty of free space on the MWCNT surface in the first place, but as the contact time increases, the active sites required for dye adsorption are filled with dye molecules and decreased. A similar situation was observed in the sorption removal of cationic dyes from aquatic solution using magnetic MWCNT by Song, Shi, et al., [15].

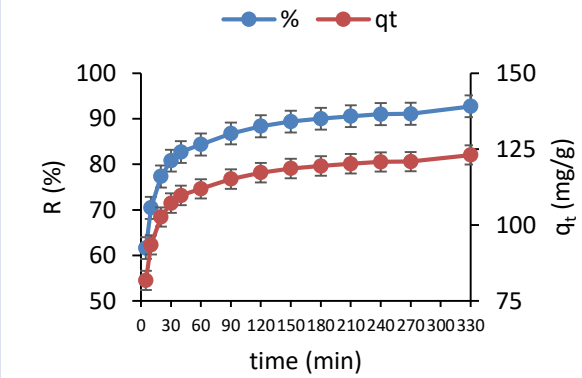

Figure 7. Impact of contact time on removal efficiency and adsorption capacity.

Effect of initial pH

The pH of the solution is a crucial factor in adsorption since it has a significant impact on the degree of ionization, the structure of the dye molecules, and the surface charge of the adsorbents [16]. Therefore, to determine the effect of solution pH on the adsorption capacity of MWCNT used as an adsorbent, the pH value was varied between 2-12 and its effect on AV 17 removal was monitored (Figure 8). The results in Figure 8 show that the amount of AV 17 adsorption by MWCNT did not significantly increase with increasing pH. While q_e was 122.53 mg/g in the solution adjusted to pH 6, this value was calculated as 126.32 mg/g at pH 12. The treatment efficiency increased from 92.32% to 95.18% when the pH increased from 6 to 12. Therefore, it was decided that it was appropriate to work at the natural pH value of the dye solution without pH adjustment.

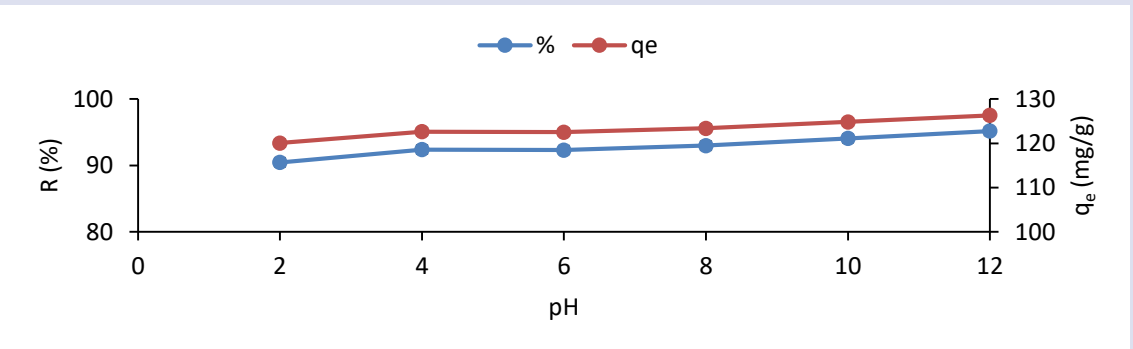

Figure 8. Effect of pH on adsorption capacity and removal efficiency.

Effect of temperature

Temperature is one of the parameters that significantly affect the sorption capacity of sorbents. The effect of temperature on AV 17 adsorption was studied at four different temperature values (25, 35, 45, and 55°C) (Figure 9). As seen in Figure 9, the adsorption efficiency and capacity increased with increasing temperature. Because high temperatures can expand the pores and/or activate the adsorbent surface [17].

Considering the cost increase that will occur if the process water temperature is increased, the process can be operated without the need for heating, especially at low concentrations, but it is more appropriate to heat the process water to the range of 35-45°C at higher dye concentrations for treatment efficiency. The increase in efficiency with increasing temperature indicates the presence of an endothermic reaction between AV 17 and MWCNT.

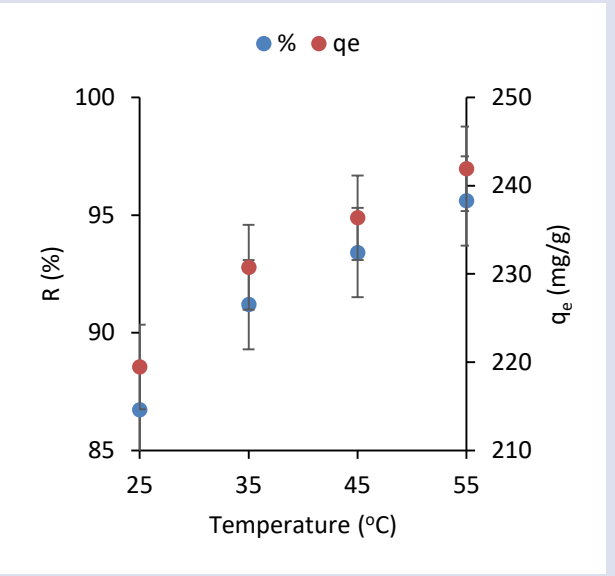

Figure 9. Effect of temperature on adsorption capacity and removal efficiency.

Adsorption kinetics

Adsorption kinetic models were used to investigate their interaction and to evaluate the mass transfer of AV 17 dye on MWCNT. To determine the contact time required to complete the adsorption process, the time range of 0-330 min was studied. Adsorption kinetic models provide important information needed to model the adsorption process, predict its rate, and design it. The adsorption kinetics of AV 17 dye with MWCNT adsorbent were investigated according to the pseudo-second-order kinetics (Figure 10a), intraparticle diffusion (Figure 10b), and Elovich (Figure 10c) models. The kinetic parameters were calculated by substituting the data obtained from Figure 7 into the equations given in Table 2. As seen in Table 2, a higher R^2 value (0.9998) was obtained for the pseudo-second-order reaction kinetics model. It is also seen that the calculated theoretical q_e value ($q_{e,cal}$) is close to the experimental q_e value ($q_{e,exp}$).

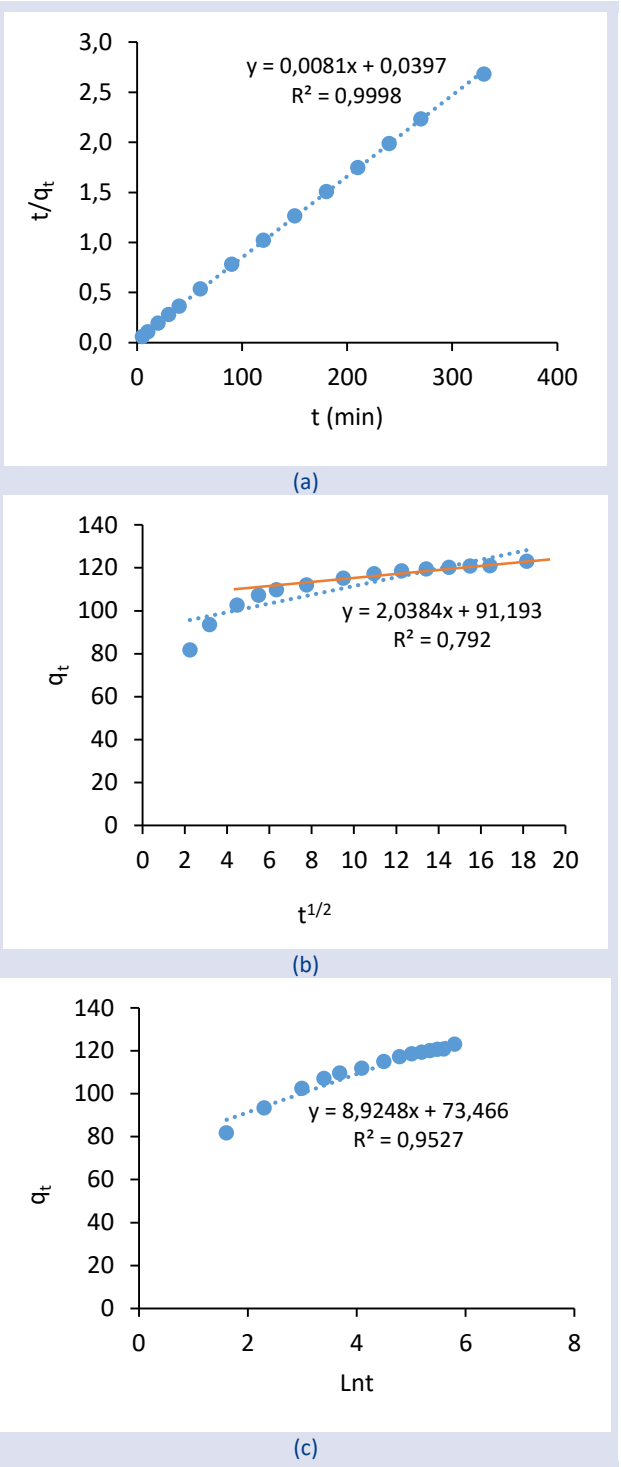

Figure 10. (a) Pseudo-second order kinetics model, (b) Intraparticle diffusion model, (c) Elovich model.

To investigate the stepwise adsorption process and analyze the diffusion mechanism, the intraparticle diffusion model was applied and the obtained graph is given in Figure 10(b). From Figure 10(b), it can be seen that the straight line between q_t and $t^{1/2}$ is nonlinear from the origin and the AV 17 adsorption of MWCNT adsorbent consists of a two-step process. The first stage's quick rise is an instantaneous diffusion of the adsorption stage at the outermost surface. The intraparticle diffusion mechanism regulates the rate during the second step, which is the progressive adsorption stage [21].

Table 2. Kinetic parameters for the adsorption of AV 17 on MWCNT

Kinetic Models	Equations		Reference
Pseudo-second-order model	$t/q_t = (1/k_2 \cdot q_e^2) + (t/q_e)$	(3)	[18]
	q_e (mg/g)	$q_{e,cal}$ = 123.45 $q_{e,exp}$ = 119.45	
	k_2 (mg/g.dk)	$1.652*10^{-3}$	
	R^2	0.9998	
Intraparticle diffusion model	$q_t = (k_d.t^{1/2}) + C$	(4)	[19]
	k_d (mg/(g $dk^{1/2}$))	2.0384	
	C (mg/g)	91.193	
	R^2	0.7920	
Elovich model	$q_t = (1/\beta).(\ln(\alpha\beta)) + (1/\beta).(\ln t)$	(5)	[20]
	α (mg/g dk)	33554.47	
	β (g/mg)	0.112	
	R^2	0.9527	

As a result, both phases work together to control the adsorption rate; intraparticle diffusion is not the only step that limits the rate. The slope of the second step is smaller than the slope of the first. This could be connected to the reduction in active sites on MWCNT that occurs as dye molecules diffuse over longer times [15].

Adsorption isotherms

The relationship between the amount of pollutant adsorbed on the adsorbent and the concentration of the pollutant in the solution at equilibrium can be explained using adsorption isotherms. Adsorption isotherm analysis is a vital tool for figuring out an adsorbent's maximal adsorption capacity. Isotherm models are used to determine the adsorption capacity as well as the physical or chemical nature of the adsorption process. In this study, Langmuir, Freundlich, and Temkin isotherm models were used to assess the adsorption data and explain the adsorption mechanism.

The Langmuir isotherm assumes that once a pore on the adsorbent surface is filled, no further sorption will occur there. The Langmuir model is a theoretical model of monolayer chemical adsorption [22]. To discover the equilibrium distribution between solid and liquid, employ the Langmuir adsorption isotherm. The Langmuir isotherm equation is given in Equation 6 and the graph formed from this equation is represented in Figure 11(a).

$$q_e = \frac{q_m \times K_L \times C_e}{1 + K_L \times C_e} \quad (6)$$

Where,

q_e: Amount of pollutant adsorbed per unit weight of adsorbent at equilibrium (mg/g),

K_L: Constant connected to the free energy of adsorption (L/mg),

q_m: Maximum capacity for adsorption (mg/g),

C_e: Concentration of pollutants in solution at the equilibrium time (mg/L).

According to the Freundlich isotherm, adsorption processes take place on heterogeneous surfaces. The concentration of the pollutant adsorbed on the adsorbent surface increases as the concentration of the pollutant in the solution increases. Equation 7 provides the Freundlich isotherm equation, and Figure 11(b) shows the graph that results from this equation.

$$q_e = K_F.C_e^{\frac{1}{n}} \quad (7)$$

Where,

K_F: Constant showing the adsorbent's adsorption capability ($mg^{1-(1/n)}L^{1/n}g^{-1}$),

n: A constant that represents the intensity of adsorption,

C_e: Concentration of the substance left in solution following adsorption (mg/L).

The heat of adsorption is inversely proportional to the increasing adsorbent surface, and the energy distribution is uniform up to the maximal binding energy of adsorption, according to the Temkin isotherm model [21]. This isotherm considers the interaction between adsorbent and adsorbate and ignores extremely high and low concentration values. This model states that the heat of adsorption (ΔH, a function of temperature) of all molecules in the layer drops linearly, not logarithmically, as the surface area of the adsorbent grows. This adsorption isotherm model covers only the intermediate concentration range [23]. Equation 8 provides the Temkin isotherm equation, and Figure 11(c) shows the graph that results from this equation.

$$q_e = B \ln (A\, C_e) \quad (8)$$

Where,

q_e: Quantity of adsorbate adsorbed at equilibrium (mg/g),

C_e: Concentration of solution at equilibrium (mg/L),

B: Constant connected to the adsorption heat (B= RT/b)

b: Temkin constant connected to the adsorption heat (J/mol), T: Absolute temperature (K), R: Gas constant (8.314 J/mol K),

A: Temkin isotherm constant (L/g).

Table 3. lists the model constants and correlation coefficients that were determined using isotherm plots. The adsorption fits the Langmuir isotherm model (R^2 = 0.9813) when the correlation coefficient values listed in Table 3 are analyzed. This demonstrates that the monolayer adsorption mechanism is the mode of adsorption.

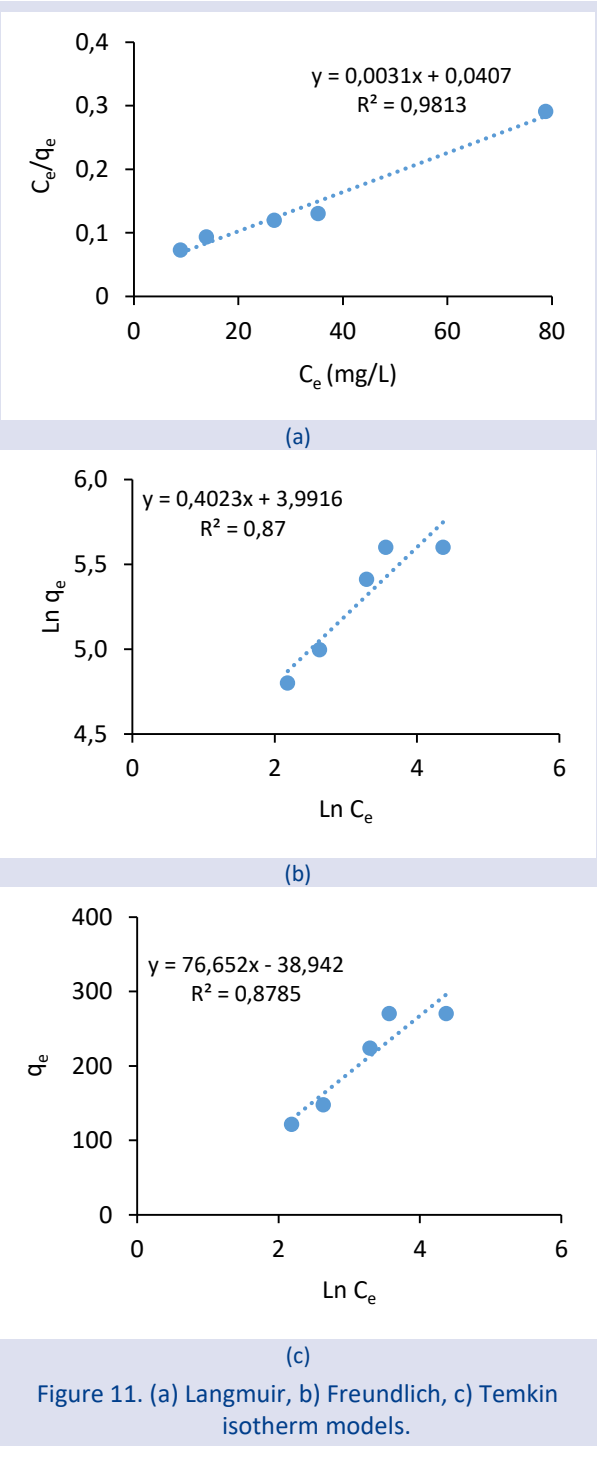

Figure 11. (a) Langmuir, b) Freundlich, c) Temkin isotherm models.

$$R_L = 1/(1+bC_o) \quad (9)$$

The varied distribution of dye molecules on the adsorption sites could be the cause of this. Equation 9 provides the calculation of R_L, a dimensionless constant derived from the Langmuir model. $0<R_L<1$: Favorable and spontaneous adsorption, $R_L>1$: Not favorable adsorption, $R_L=1$: The linear process, $R_L=0$: Irreversible adsorption [24].

Where C_o is the initial dye concentration.

Since the R_L value was obtained in the range of 0 to 1 for all dye concentrations (0.116 for 100 mg/L AV 17; 0.042 for 300 mg/L AV 17), it can be concluded that the adsorption process is effective in removing AV 17 dye and a strong bond is formed between MWCNT and dye. Table 3 displays the coefficients of adsorption intensity (n) and adsorption capacity (K_F) that were determined using the Freundlich model.

The n should take values ranging from 1 to 10 for a preferable adsorption process. Furthermore, n>1 denotes the formation of multiple layers on the adsorbent surface. The 1/n represents the surface heterogeneity factor. Surface heterogeneity rises as 1/n gets closer to zero [25]. When we look at Table 3, the n value determined from the Freundlich model is 2.485 and the 1/n value is 0.4. This indicates that AV 17 adsorption on the adsorbent is preferred and the MWCNT adsorbent surface is heterogeneous.

Table 3. Isotherm parameters for the adsorption of AV 17 on MWCNT

Langmuir	q_m (mg/g)	b (L/mg)	R^2
	322,58	0,076	0,9813
Freundlich	K_F (mg/g)	n ((mg/g)·(L/mg)$^{1/n}$)	R^2
	54,14	2,485	0,87
Temkin	A (L/g)	B (J/mol)	R^2
	0,6	76,652	0,8785

Furthermore, the n value is employed to denote the chemical or physical nature of the process. In chemical processes, n<1 denotes whereas in physical processes, n≥1 [26]. The physical mechanism was responsible for the realization of AV 17 adsorption on MWCNT, as indicated by the n constant (2.485) obtained for this work.

Table 4. compares the maximal Langmuir adsorption capacities (q_{max} (mg/g)) of MWCNT for the adsorption of different pollutants. Table 4 confirms that this nanocomposite is an effective applicant for AV 17 dye-containing wastewater treatment. When compared with other adsorbate materials to be treated, it is seen that higher efficiency per unit adsorbent is obtained from this study. In their study, Moussavi and Fazli [27] also examined Acid violet 17 dye decolorization by multi-walled carbon nanotubes from aqueous solution. However, it differs from this study in terms of working conditions, research method, and results obtained. The adsorption capacity obtained after 180 minutes of contact time at a concentration of 25 mg/L AV17 at pH 4 and a dose of 0.4 g/L MWCNT is about 4.5 mg/g. This result is considerably lower than the unit adsorption capacity obtained in this study as shown in Table 4.

Table 4. Adsorption capacities determined from the Langmuir isotherm model for different adsorbate materials uptake by MWCNT

Adsorbate material	pH	Adsorbate conc. (mg/L)	Sorbent dose (g/L)	Time	q_m (mg/g)	References
Phenol	4.65	50	2	56 min	64.60	[28]
Cr(VI)	5-6	100	0.15	6 h	24	[29]
Direct Blue 53	2	300	1.5	3 h	334.8	[30]
Congo Red		50-400	2.5		148.08	[31]
Reactive green HE4BD		50-400	2.5		151.88	[31]
Methylene blue	6	20	1.0	1 h	19.6	[32]
Golden yellow MR		50-400	2.5		141.618	[31]
Triclosan	3, 10	8	0.05		166.83	[33]
Methyl orange	2	20	0.3	2 h	50.25	[34]
Phenol Ni(II)	7	25	5	5 h	32.25 6.09	[35]
Maxilon blue dye (GRL)	6	50	0.1	2 h	187.69	[36]
Methylene Blue Dye		40-100		1 h	55.18	[37]
MB AR 183	6	10	0.2g		59.7 45.2	[38]
AV 17	6.52	200	0.8	3 h	322.58	*

Adsorption thermodynamics

Adsorption thermodynamics was examined to examine the adsorption mechanism of AV 17 on MWCNT. Table 5 presents the results of the computations for three thermodynamic parameters: the change in Gibbs free energy ($\Delta G°$), the change in enthalpy ($\Delta H°$), and the change in entropy ($\Delta S°$). From the slope ($\Delta H°$) and shift ($\Delta S°$) of the 1/T plot vs ln K_c in Figure 12, the values of $\Delta H°$ and $\Delta S°$ are computed.

$$\Delta G^o = -RT \ln K_c \quad (10)$$

$$\Delta G^o = \Delta H° - T\Delta S° \quad (11)$$

$$\ln K_c = \Delta S°/R - \Delta H°/RT \quad (12)$$

Where,
R = Universal gas constant; T = Absolute temperature (K)

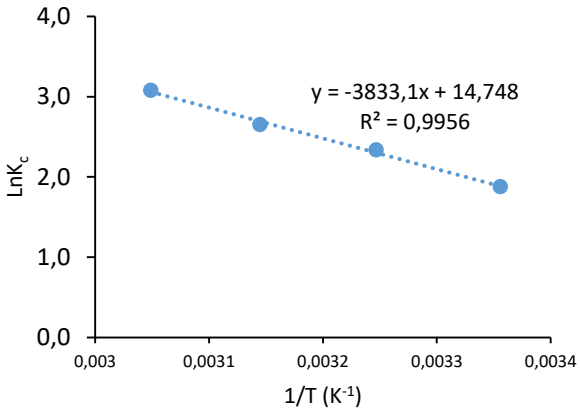

Figure 12. The estimation of thermodynamic parameters.

Table 5. Thermodynamic parameters for adsorption of AV 17 on MWCNT at different temperatures

	ΔG^o (kJ/mol)				ΔS^o (kJ/mol.K)	ΔH^o (kJ/mol)
Temperature (K)	298	308	318	328		
C_o (mg/L) 200	-4,651	-5,986	-7,010	-8,399	0,123	31,870

From Table 5., it is seen that the $\Delta G°$ value decreases as the temperature increases. Negative $\Delta G°$ values indicate that adsorption is spontaneous and thermodynamically favorable. Also, absolute values of $\Delta G°$ less than 20 kJ/mol indicate that dye adsorption on MWCNT is mainly physical adsorption. Positive $\Delta H°$ values indicate that the reaction is endothermic. In addition, an absolute $\Delta H°$ value of less than 84 kJ/mol indicates that the process is physical adsorption [39]. Positive $\Delta S°$ values are also related to the randomness of the whole system during the adsorption process and the adsorbent's AV 17 gravity force [40].

Conclusions

Many parameters such as dye concentration, pH, contact time, adsorbent dose and temperature were found to be effective in the removal of AV 17 using MWCNT. It was determined that the treatment was more effective at natural pH conditions. This is very beneficial at the application scale as there is no additional cost for pH adjustment. The kinetic and isotherm modeling of AV 17 dye adsorption with MWCNT showed agreement with pseudo-second-order kinetics and the Langmuir isotherms. The thermodynamic study presented a favorable and spontaneous adsorption process. MWCNT showed a high adsorption capacity (q_m= 322.58 mg/g). This is a very good value compared to other results obtained in the literature for AV 17 dye removal. All the results obtained showed that MWCNT can be used effectively for azo group dye removal.

Conflicts of interest

There are no conflicts of interest in this work.

References

[1] Saleem M., Pirzada T., Qadeer R., Sorption of Some Azo-Dyes on Wool Fiber from Aqueous Solutions, *Colloids Surf. A: Physicochem. Eng. Asp.,* 260 (1–3) (2005) 183–188.

[2] Saleem M., Pirzada T., Qadeer R., Sorption of Acid Violet 17 and Direct Red 80 Dyes on Cotton Fiber from Aqueous Solutions, *Colloids Surf. A: Physicochem. Eng. Asp.,* 292 (2–3) (2007) 246–250.

[3] Jain S.N., Gogate P.R., Adsorptive Removal of Acid Violet 17 Dye from Wastewater Using Biosorbent Obtained from NaOH and H_2SO_4 Activation of Fallen Leaves of *Ficus racemosa*, *J. Mol. Liq.*, 243 (2017) 132–143.

[4] Kodavatiganti S., Bhat A.P., Gogate P.R., Intensified Degradation of Acid Violet 7 Dye using Ultrasound Combined with Hydrogen Peroxide, Fenton, and Persulfate, *Sep. Purif. Technol.,* 279 (2021) 119673.

[5] Jain S.N., Shaikh Z., Mane V.S., Vishnoi S., Mawal V.N., Patel O.R., et al., (2019) Nonlinear Regression Approach for Acid Dye Remediation Using Activated Adsorbent: Kinetic, Isotherm, Thermodynamic and Reusability Studies, *Microchem J.,* 148 (2019) 605–615.

[6] Üstün-Odabaşı S., Utilizing Sustainable Hemp Biomass as an Eco-Friendly for Potentially Toxic Elements Removal from Water, *Mater. Res. Express*, 11 (2) (2024) 025104.

[7] Şentürk İ., Alzein M., Adsorption of Acid Violet 17 onto Acid-Activated Pistachio Shell: Isotherm, Kinetic and Thermodynamic Studies, *Acta Chim. Slov.,* 67(1) (2020) 55–69.

[8] Jain S.N., Gogate P.R., Adsorptive Removal of Acid Violet 17 Dye from Wastewater using Biosorbent Obtained from NaOH and H_2SO_4 Activation of Fallen Leaves of *Ficus Racemosa*, *J. Mol. Liq.,* 243 (2017) 132–143.

[9] Thinakaran N., Baskaralingam P., Pulikesi M., Panneerselvam P., Sivanesan S., Removal of Acid Violet 17 from Aqueous Solutions by Adsorption onto Activated Carbon Prepared from Sunflower Seed Hull, *J. Hazard. Mater.*, 151 (2) (2008) 316–322.

[10] Gupta V.K., Agarwal S., Bharti A.K., Sadegh H., Adsorption Mechanism of Functionalized Multi-Walled Carbon Nanotubes for Advanced Cu (II) Removal, *J. Mol. Liq.,* 230 (2017) 667–673.

[11] Al-Johani H., Salam M.A., Kinetics and Thermodynamic Study of Aniline Adsorption by Multi-Walled Carbon Nanotubes from Aqueous Solution, *J. Colloid Interface Sci.,* 360 (2), (2011) 760–767.

[12] Zhou W., Zhou X., Song W., Wang C., Zhang H., Huang X., Removal of Benzohydroxamic Acid from Aqueous Solutions using Multi-Walled Carbon Nanotubes/Iron-Doped Hydroxyapatite Composites: Synthesis, Adsorption Performance, and Characteristics, *J. Environ. Chem. Eng.*, 11 (6) (2023) 111259.

[13] Topal Canbaz G., Fe_3O_4@Granite: A Novel Magnetic Adsorbent for Dye Adsorption, *Processes*, 11 (9) (2023) 2681.

[14] Egbosiuba T.C., Egwunyenga M.C., Tijani J.O., Mustapha S., Abdulkareem A.S., Kovo A.S., et al., Activated Multi-Walled Carbon Nanotubes Decorated with Zero Valent Nickel Nanoparticles for Arsenic, Cadmium and Lead Adsorption from Wastewater in a Batch and Continuous Flow Modes, *J. Hazard. Mater.*, 423 (2022) 126993.

[15] Song G., Shi Y., Wang H., Li A., Li W., Sun Y., et al., Effective Sorptive Removal of Five Cationic Dyes from Aqueous Solutions by Using Magnetic Multi-Walled Carbon Nanotubes, *Water Sci. Technol.*, 85 (7) (2022) 1999–2014.

[16] Song G., Tong L., Chen S., Zhang J., Zhang Y., Wang H., et al., Facile Fabrication of Amino Functionalized Magnetic Multi-walled Carbon Nanotubes for Removal of Congo Red from Aqueous Solutions, *Water Air Soil Pollut.,* 233 (12) (2022) 534.

[17] Abutaleb A., Imran M., Zouli N., Khan A.H., Hussain S., Ali M.A., et al., Fe_3O_4-Multiwalled Carbon Nanotubes-Bentonite as Adsorbent for Removal of Methylene Blue from Aqueous Solutions, *Chemosphere*, 316 (2023) 137824.

[18] Ho Y.S., McKay G., Pseudo-Second Order Model for Sorption Processes, *Process Biochem.*, 34 (5) (1999) 451–465.

[19] Weber W.J., Morris J.C., Kinetics of Adsorption on Carbon from Solution, *J. Sanit. Eng. Div.,* 89 (2) (1963) 31–60.

[20] Chien S.H., Application of Elovich Equation to the Kinetics of Phosphate Release and Sorption in Soils, *Soil Sci. Soc. Am. J.,* 44 (2) (1980) 265–268.

[21] Balarak D., McKay G., Utilization of MWCNTs/Al_2O_3 as Adsorbent for Ciprofloxacin Removal: Equilibrium, Kinetics and Thermodynamic Studies, *J. Environ. Sci. Health A Tox., Part A*, 56 (3) (2021) 324–333.

[22] Wang J., Guo X., Adsorption Isotherm Models: Classification, Physical Meaning, Application and Solving Method, *Chemosphere*, 258 (2020) 127279.

[23] Edet U.A., Ifelebuegu A.O., Kinetics, Isotherms, and Thermodynamic Modeling of the Adsorption of Phosphates from Model Wastewater Using Recycled Brick Waste, *Processes*, 8 (6) (2020) 665.

[24] Chandrasekaran A., Patra C., Narayanasamy S., Subbiah S., Adsorptive Removal of Ciprofloxacin and Amoxicillin from Single and Binary Aqueous Systems using Acid-Activated Carbon from *Prosopis juliflora*, *Environ. Res.*, 188 (2020) 109825.

[25] Şentürk İ., Yıldız M.R., Highly Efficient Removal from Aqueous Solution by Adsorption of Maxilon Red GRL dye using Activated Pine Sawdust, *Korean J. Chem. Eng.*, 37 (6) (2020) 985–999.

[26] Şentürk İ., Effective Adsorption of Congo Red by Eco-Friendly Granite-Modified Magnetic Chitosan Nanocomposite (G@Fe3O4@CS), *Biomass Conv. Bioref.,* (2023) *https://doi.org/10.1007/s13399-023-04826-1*

[27] Moussavi S.P., Mohammadian Fazli M., Acid Violet 17 Dye Decolorization by Multi-walled Carbon Nanotubes from Aqueous Solution, *JHEHP*, 1 (2) (2016) 110–117.

[28] Dehghani M.H., Mostofi M., Alimohammadi M., McKay G., Yetilmezsoy K., Albadarin A.B., et al., High-Performance Removal of Toxic Phenol by Single-Walled and Multi-Walled Carbon Nanotubes: Kinetics, Adsorption, Mechanism and Optimization Studies, *J. Ind. Eng. Chem.*, 35 (2016) 63–74.

[29] Ahmadpour A., Eftekhari N., Ayati A., Performance of MWCNTs and a Low-Cost Adsorbent for Chromium (VI) Ion Removal, *J. nanostructure chem.*, 4 (2014) 171–178.

[30] Prola L.D., Machado F.M., Bergmann C.P., de Souza F.E., Gally C.R., Lima E.C., et al., Adsorption of Direct Blue 53 Dye from Aqueous Solutions by Multi-Walled Carbon Nanotubes and Activated Carbon, *J Environ Manage.,* 130 (2013) 166–175.

[31] Mishra A.K., Arockiadoss T., Ramaprabhu S., Study of Removal of Azo Dye by Functionalized Multi Walled Carbon Nanotubes, *Chem. Eng. J.*, 162 (3) (2010) 1026–1034.

[32] Ahmed S.H., Rasheed E.A.A., Rasheed, L.A.A., Abdulrahim, F.R. Decolorization of Cationic Dye from Aqueous Solution by Multiwalled Carbon Nanotubes, *J. Ecol. Eng.*, 25 (2) (2024) 72–84.

[33] Zhou S., Shao Y., Gao N., Deng J., Tan C., Equilibrium, Kinetic, and Thermodynamic Studies on the Adsorption of Triclosan onto Multi-Walled Carbon Nanotubes, *Clean - Soil Air Water*, 41 (6) (2013) 539–547.

[34] Yao Y., Bing H., Feifei X., Xiaofeng C., Equilibrium and Kinetic Studies of Methyl Orange Adsorption On Multiwalled Carbon Nanotubes, *Chem Eng J.,* 170 (1) (2011) 82–89.

[35] Abdel-Ghani N.T., El-Chaghaby G.A., Helal F.S., Individual and Competitive Adsorption of Phenol and Nickel onto Multiwalled Carbon Nanotubes, *J. Adv. Res.*, 6 (3) (2015) 405–415.

[36] Alkaim A.F., Sadik Z., Mahdi D.K., Alshrefi S.M., Al-Sammarraie A.M., Alamgir F.M., et al., Preparation, Structure and Adsorption Properties of Synthesized Multiwall Carbon Nanotubes for Highly Effective Removal of Maxilon Blue Dye, *Korean J. Chem. Eng.,* 32 (2015) 2456–2462.

[37] Ceroni L., Benazzato S., Pressi S., Calvillo L., Marotta E., Menna E., Enhanced Adsorption of Methylene Blue Dye on Functionalized Multi-Walled Carbon Nanotubes, *Nanomaterials*, 14 (6) (2024) 522.

[38] Wang S., Ng C.W., Wang W., Li Q., Hao Z., Synergistic and Competitive Adsorption of Organic Dyes on Multiwalled Carbon Nanotubes, *Chem. Eng. J.*, 197 (2012) 34–40.

[39] Lin R., Liang Z., Yang C., Zhao Z., Cui F., Selective Adsorption of Organic Pigments on Inorganically Modified Mesoporous Biochar and Its Mechanism Based on Molecular Structure, *J. Colloid Interface Sci.*, 573 (2020) 21–30.

[40] Şentürk İ., Şartlandırılmış Zeolit - Klinoptilolit Minerali ile Bakır Gideriminin Araştırılması, *Karadeniz Fen Bilimleri Dergisi*, 13 (1) (2023) 97–113.